On the Distribution of Zeros of Mobile Channels with Application to GSM/EDGE

Robert Schober, *Student Member, IEEE,* and Wolfgang H. Gerstacker, *Member, IEEE*

***Abstract*—In this paper, the distribution of zeros of mobile channels is investigated and the results obtained are applied to the GSM/EDGE system. The taps of the discrete-time overall impulse response can be modeled as correlated complex Gaussian random variables, where the correlations depend on the transmit filter, the power delay profile of the channel, and the receiver input filter. For calculation of the density of zeros of the overall transfer function, a result from the mathematical literature is used. From this density, two cumulative distributions which are relevant for the design of suboptimum receivers are derived. Our investigations show that for the power delay profiles specified for GSM/EDGE, an allpass prefilter which transforms the impulse response in its minimum phase equivalent should be employed if decision-feedback equalization (DFE) or reduced-state sequence estimation (RSSE) are used at the receiver. On the other hand, if impulse response truncation using a linear prefilter is applied, the truncated impulse response should have a length of three as will be shown.**

***Index Terms*—Equalization, GSM/EDGE, mobile channels, random polynomials, statistical characterization.**

I. Introduction

TYPICALLY, FOR THE DESIGN of digital receivers the discrete-time overall channel is modeled as a finite impulse response (FIR) filter resulting from symbol-spaced sampling of the continuous-time receiver input signal. Here, the discrete-time overall impulse response depends on the impulse response of transmit filter, continuous-time equivalent baseband channel, and receiver input filter. As long as the overall channel is flat, receiver design is relatively simple; however, for frequency-selective channels, sophisticated equalizers are necessary. If optimum maximum-likelihood sequence estimation (MLSE) [1], [2], employing a full-state Viterbi algorithm (VA) [3] is used in the receiver, the minimum Euclidean distance associated with the discrete-time impulse response is the most important parameter for receiver performance. However, in many situations where the allowable computational complexity is limited which is, e.g., the case in mobile communications[1] [6], [5] suboptimum equalization strategies such as delayed decision-feedback sequence estimation (DDFSE) [7] or reduced-state sequence estimation (RSSE) [8], impulse response truncation using a prefilter before the VA [9]–[14], decision-feedback equalization (DFE) [15], or even linear equalization (LE) [16] have to be employed. For these suboptimum receivers, the location of the zeros of the z-transform of the discrete-time overall channel impulse response is very important. For example, LE does not perform well if zeros are located close to the unit circle of the complex plane, whereas DFE and DDFSE/RSSE degrade if zeros are located outside the unit circle, i.e., if the discrete-time impulse response is not minimum phase.

For static channels, which may be found, e.g., in cable transmission [19], the zeros of the impulse response are known in advance and the receiver can be designed accordingly. In mobile communications, however, the channel is time-variant due to the motion of the mobile station, i.e., the overall impulse response is not known *a priori*. In many cases, the equivalent baseband channel impulse response can be modeled as a sum of delayed Dirac delta impulses [20]. Each Dirac pulse corresponds to one propagation path and is weighted with a complex-valued random amplitude. Usually, these amplitudes are assumed to be mutually independent zero-mean complex Gaussian random variables. Such channels are characterized by their power delay profile [20]. The coefficients of the resulting discrete-time overall impulse response are correlated Gaussian random variables. Clearly, for mobile channels, the location of the zeros of the overall transfer function is also random and the receiver cannot be designed for one particular channel. However, the *distribution* of the zeros of the overall impulse response which is influenced by the transmit filter, the power delay profile of the mobile channel, the receiver input filter, and the sampling phase, can provide important information for receiver design as will be shown in detail.

This paper is organized as follows. In Section II, the covariance matrix of the impulse response coefficients is calculated as a function of transmit filter, power delay profile, receiver input filter, and sampling phase. In Section III, we apply a result from the mathematical literature [21] (cf. also [22]) and calculate the density of zeros in the complex plane for an overall transfer function whose coefficients are correlated complex Gaussian

Manuscript received November 28, 1999; revised February 14, 2001. This work was supported by Technology Center for Mobile Communication (TCMC), Philips Semiconductors, Germany. This paper was presented in part at the IEEE International Symposium on Personal, Indoor and Mobile Communication (PIMRC), London, U.K., September 2000, and the IEEE International Conference on Communications (ICC), Helsinki, Finland, June 2001.

R. Schober was with the Telelcommunications Laboratory, University of Erlangen-Nurnberg, D-91058 Erlangen, Germany. He is now with the Department of Electrical and Computer Engineering, University of Toronto, Toronto, ON M5S 1A1, Canada (e-mail: rschober@comm.utoronto.ca).

W. Gerstacker is with the Telecommunications Laboratory, University of Erlangen-Nurnberg, D-91058 Erlangen, Germany.

Publisher Item Identifier S 0733-8716(01)04711-4.

[1]Note that computational complexity of MLSE might not be a major problem for Global System for Mobile Communications (GSM) where a binary modulation format is used, i.e., if a maximum channel length of seven is assumed, the VA requires $2^6 = 64$ states. For enhanced data rates for GSM evolution (EDGE) [4], however, where eight-ary phase-shift keying is employed, the same channel length implies $8^6 = 262\,144$ states which is currently much too complex for implementation [5].

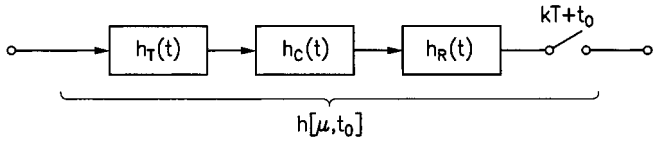

Fig. 1. Block diagram of the equivalent baseband continuous-time transmission model.

random variables. Two cumulative distribution functions are derived from the density and their relevance for receiver (equalizer) design is discussed in Section IV. Also in this section, the special case of uncorrelated impulse response coefficients is considered. Some results for the power delay profiles [4] specified for GSM and EDGE [23] are shown in Section V. Finally, Section VI concludes this work.

II. Correlation Matrix of the Coefficients of the Overall Impulse Response

A block diagram of the equivalent baseband continuous-time transmission model is shown in Fig. 1. Here, $h_T(t)$ and $h_R(t)$ denote the transmit and the receiver input filter impulse response, respectively. $h_C(t)$ is the (random) equivalent baseband channel impulse response. Usually, $h_C(t)$ is characterized by its power delay profile [20]

$$P(t) = \sum_{\nu=0}^{N-1} \sigma_\nu^2 \, \delta(t - \tau_\nu) \tag{1}$$

where N, σ_ν^2, and τ_ν, $0 \le \nu \le N-1$, denote the number of different paths, the variance, and the delay of path ν, respectively. $\delta(\cdot)$ is the Dirac delta function [17]. $h_C(t)$ may be modeled as

$$h_C(t) = \sum_{\nu=0}^{N-1} g_\nu \, \delta(t - \tau_\nu) \tag{2}$$

with mutually independent coefficients g_ν, $0 \le \nu \le N-1$, i.e.,

$$\mathcal{E}\{g_\nu g_\mu^*\} = \begin{cases} \sigma_\nu^2, & \nu = \mu \\ 0, & \nu \neq \mu \end{cases} \tag{3}$$

[$\mathcal{E}\{\cdot\}$ and $(\cdot)^*$ denote expectation and complex conjugation, respectively]. To avoid mathematical problems, the coefficients g_ν are assumed to be time-invariant. Such a model is valid for example for burst transmission and low vehicle speeds. In this case, g_ν is approximately constant during one burst but varies from burst to burst. For high vehicle speeds, this simple model is no longer valid; however, the results concerning the distribution of the zeros of the overall impulse response obtained in this paper are still applicable.

The overall continuous-time impulse response $h(t)$ is given by

$$h(t) \triangleq h_T(t) * h_C(t) * h_R(t) \tag{4}$$

where $*$ denotes convolution. Using the combined impulse response of transmit and receiver input filter

$$h_G(t) \triangleq h_T(t) * h_R(t) \tag{5}$$

the overall impulse response $h(t)$ can be calculated to

$$\begin{aligned} h(t) &= h_G(t) * h_C(t) \\ &= \sum_{\nu=0}^{N-1} g_\nu h_G(t - \tau_\nu). \end{aligned} \tag{6}$$

The received signal is sampled at times $kT + t_0$, where $k \in \mathbb{Z}$, T, and t_0 denote discrete time, symbol duration, and sampling phase, respectively. The discrete-time overall impulse response $h[\mu, t_0]$ ($\mu \in \mathbb{Z}$ denotes the coefficient number) can be written as

$$\begin{aligned} h[\mu, t_0] &\triangleq h(\mu T + t_0) \\ &= \sum_{\nu=0}^{N-1} g_\nu h_G(\mu T + t_0 - \tau_\nu). \end{aligned} \tag{7}$$

Obviously, the discrete-time overall impulse response depends on the sampling phase t_0 which has to be chosen properly. The energy $E(t_0)$ of $h[\mu, t_0]$ is

$$\begin{aligned} E(t_0) &\triangleq \mathcal{E}\left\{ \sum_{\mu=-\infty}^{\infty} |h[\mu, t_0]|^2 \right\} \\ &= \sum_{\mu=-\infty}^{\infty} \sum_{\nu=0}^{N-1} \sigma_\nu^2 \, |h_G(\mu T + t_0 - \tau_\nu)|^2 \end{aligned} \tag{8}$$

where (3) is used. Usually, the discrete-time overall impulse response can be truncated to a finite length L. L should be chosen large enough in order to make the precursor energy

$$E_{\text{pre}}(t_0) \triangleq \mathcal{E}\left\{ \sum_{\mu=-\infty}^{-1} |h[\mu, t_0]|^2 \right\} \tag{9}$$

and the postcursor energy

$$E_{\text{post}}(t_0) \triangleq \mathcal{E}\left\{ \sum_{\mu=L}^{\infty} |h[\mu, t_0]|^2 \right\} \tag{10}$$

negligible. One reasonable criterion to determine an appropriate sampling phase t_0 is to maximize the energy contained in $h[\mu, t_0]$, $0 \le \mu \le L-1$:

$$\hat{t}_0 = \arg\max_{t_0} \{E_L(t_0)\} \tag{11}$$

where $E_L(t_0)$ is defined as

$$\begin{aligned} E_L(t_0) &\triangleq \mathcal{E}\left\{ \sum_{\mu=0}^{L-1} |h[\mu, t_0]|^2 \right\} \\ &= \sum_{\mu=0}^{L-1} \sum_{\nu=0}^{N-1} \sigma_\nu^2 \, |h_G(\mu T + t_0 - \tau_\nu)|^2 . \end{aligned} \tag{12}$$

Note that in a real transmission system where the sampling phase may have to be estimated in every burst, $\hat{t}_0$ may be different from burst to burst for a given power delay profile. However, our investigations showed that $\hat{t}_0$ varies only slightly as long as L is chosen properly and in this case the influence of this effect on the distribution of zeros is negligible. We would like to emphasize that if L is chosen too large, the first and/or the last taps of the discrete-time overall impulse response contain very little energy which leads to additional zeros with very large and/or very small magnitudes.

Once $\hat{t}_0$ has been determined, the overall transfer function $H(z, \hat{t}_0)$, $z \in \mathbb{C}$, i.e., the z-transform of the discrete-time overall impulse response, can be calculated to [18]

$$\begin{aligned} H(z, \hat{t}_0) &= \sum_{\mu=0}^{L-1} h[\mu, \hat{t}_0] z^{-\mu} \\ &= z^{-(L-1)} \sum_{\mu=0}^{L-1} h[L-1-\mu, \hat{t}_0] z^{\mu} \\ &= z^{-(L-1)} \boldsymbol{h}^T(\hat{t}_0) \boldsymbol{v}(z) \end{aligned} \tag{13}$$

where $(\cdot)^T$ denotes transposition and the definitions

$$\boldsymbol{h}(\hat{t}_0) \triangleq \left[h[L-1, \hat{t}_0] h[L-2, \hat{t}_0] \cdots h[0, \hat{t}_0]\right]^T \tag{14}$$

$$\boldsymbol{v}(z) \triangleq [1 z \cdots z^{L-1}]^T \tag{15}$$

are used.

In the next section, the density of the zeros of $H(z, \hat{t}_0)$ in the complex plane will be calculated. For this, the covariance matrix

$$\boldsymbol{C}(\hat{t}_0) \triangleq \mathcal{E}\{\boldsymbol{h}(\hat{t}_0) \boldsymbol{h}^H(\hat{t}_0)\} \tag{16}$$

[$(\cdot)^H$ denotes Hermitian transposition] of coefficient vector $\boldsymbol{h}(\hat{t}_0)$ has to be determined. For simplicity of notation, we replace $\boldsymbol{C}(\hat{t}_0)$ by $\boldsymbol{C}$ in the following. Using (3), (7), and (16), the elements $c_{\mu\nu}$, $0 \le \mu, \nu \le L-1$, of $\boldsymbol{C}$ can be calculated to

$$\begin{aligned} c_{\mu\nu} &\triangleq \mathcal{E}\left\{h[L-1-\mu, \hat{t}_0] h^*[L-1-\nu, \hat{t}_0]\right\} \\ &= \sum_{\xi=0}^{N-1} \sigma_\xi^2 h_G\left((L-1-\mu)T + \hat{t}_0 - \tau_\xi\right) \\ &\quad h_G^*\cdot\left((L-1-\nu)T + \hat{t}_0 - \tau_\xi\right). \end{aligned} \tag{17}$$

III. Density of Zeros of the Overall Transfer Function

In [21], the more general problem of calculating the distribution of the zeros of a system of equations is addressed. If we specialize [21, Theorem 8.1] to the problem at hand, the expected number $N_{\mathcal{U}}$ of zeros of the overall transfer function $H(z, \hat{t}_0)$ that lie in the set (region) $\mathcal{U}$ is

$$N_{\mathcal{U}} = \int_{\mathcal{U}} f_z(z)\, dx\, dy \tag{18}$$

where x and y denote the real and the imaginary part of $z = x + jy$, respectively, while

$$f_z(z) \triangleq \frac{1}{\pi} \frac{\partial^2}{\partial z \partial z^*} \log\left(\boldsymbol{v}(z)^T \boldsymbol{C} \boldsymbol{v}(z^*)\right) \tag{19}$$

is referred to as the *density* of zeros in the complex plane [21]. Note that $\log(\boldsymbol{v}(z)^T \boldsymbol{C} \boldsymbol{v}(z^*))$ is not a holomorphic function, of course. For the density $f_z(z) \ge 0$, $\forall z$, is valid and thus, $\log(\boldsymbol{v}(z)^T \boldsymbol{C} \boldsymbol{v}(z^*))$ is a subharmonic function [24].

As shown in the Appendix, $f_z(z)$ may be calculated to

$$f_z(z) \triangleq \frac{1}{\pi |z|^2} \left(\frac{l_1(z)}{l_0(z)} - \left(\frac{|l_2(z)|}{l_0(z)}\right)^2\right) \tag{20}$$

with the definition

$$l_\xi(z) \triangleq \boldsymbol{v}(z)^T \boldsymbol{C}_\xi \boldsymbol{v}(z^*), \qquad \xi = 0, 1, 2. \tag{21}$$

The elements $c_{\mu\nu}[\xi]$, $0 \le \mu, \nu \le L-1$, of matrices $\boldsymbol{C}_\xi$ are given by

$$c_{\mu\nu}[0] = c_{\mu\nu} \tag{22}$$

$$c_{\mu\nu}[1] = \mu\nu c_{\mu\nu} \tag{23}$$

$$c_{\mu\nu}[2] = \mu c_{\mu\nu}. \tag{24}$$

IV. Relevant Cumulative Distributions for Equalizer Design

In this section, two cumulative distributions relevant for equalizer design are defined and calculated for the special case of a discrete-time overall impulse response with uncorrelated coefficients.

A. Relevant Cumulative Distributions

For equalizer design, the phase of the zeros of the overall transfer function is not important. The important parameter is the magnitude of the zeros. Therefore, we change to polar coordinates r, φ, i.e., $z = r \cdot e^{j\varphi}$, $0 \le r < \infty$, $0 \le \varphi < 2\pi$, is valid, and define the marginal density $f_r(r)$ [25]

$$f_r(r) \triangleq r \int_0^{2\pi} f_z\left(r\cos(\varphi) + jr\sin(\varphi)\right) d\varphi \tag{25}$$

Now, the expected number of zeros in the disc $|z| = r \le R$ is given by

$$n(R) = \int_0^R f_r(r)\, dr \tag{26}$$

where $n(R)$ is also referred to as the unnormalized cumulative distribution function of the magnitude of the zeros [21]. Here, unnormalized means that $\lim_{R\to\infty} n(R)$ yields $L-1$ (which is the total number of zeros) and not 1 as it is usual for cumulative distribution functions. For the design of reduced-state trellis-based equalizers such as DFE [15] and DDFSE/RSSE [7], [8] receivers $n(R=1)$, i.e., the expected number of zeros inside the unit circle is an important figure of merit. If zeros are located outside the unit circle, the corresponding impulse response is not minimum phase, and without minimum phase transformation a loss in performance is inevitable. Thus, if $n(R=1) \not\approx L-1$, the receiver designer should insert an allpass prefilter [26], [27].

For LE [16] and impulse response truncation for the VA using a linear prefilter [9]–[14] the expected number of zeros $d(\rho)$ inside the region $\rho \le |z| \le 1/\rho$, $0 < \rho < 1$, is of high significance. It can be obtained from

$$d(\rho) = n(1/\rho) - n(\rho) \tag{27}$$

and may also be viewed as an unnormalized cumulative distribution since $\lim_{\rho\to 1} = 0$ and $\lim_{\rho\to 0} = L-1$ are valid. LE performs bad if there are zeros close to the unit circle. Thus, if $d(\rho) \not\approx 0$ for ρ close to 1 (say $\rho = 0.9$), LE cannot be employed. Although many different prefilter optimization criteria have been proposed for impulse response truncation ([9]–[14]), the performance of these schemes is only satisfactory if the number of zeros of the truncated impulse response is not smaller than the number of zeros close to the unit circle of the orig-

inal impulse response since otherwise the prefilter enhances the channel noise considerably. Therefore, $d(\rho)$ provides important information for the proper choice of the length of the truncated impulse response.

B. Uncorrelated Impulse Response Coefficients

In general, $f_r(r)$, $n(R)$, and $d(\rho)$ have to be evaluated using numerical integration. This will be done for the parameters of the GSM/EDGE system in Section V. For the special case of uncorrelated impulse response coefficients $h[\mu, t_0]$, $0 \le \mu \le L-1$, however, closed-form results can be obtained. Although, in practice, uncorrelatedness will be fulfilled only approximately, this simple special case offers some important insights.

If the impulse response coefficients are uncorrelated, matrix $\boldsymbol{C}$ simplifies to

$$\boldsymbol{C} = \operatorname{diag}(\sigma^2_{h,\,L-1},\, \sigma^2_{h,\,L-2},\, \ldots,\, \sigma^2_{h,\,0}) \tag{28}$$

where $\operatorname{diag}(x_1, x_2, \ldots, x_S)$ denotes an $S \times S$ diagonal matrix with main diagonal elements $x_1, x_2, \ldots, x_S$ and $\sigma^2_{h,\,\mu}$, $0 \le \mu \le L-1$, is the variance of coefficient $h[\mu, \hat{t}_0]$. Thus, (20) can be simplified to

$$f_z(z) = \frac{1}{\pi |z|^2} \left(\frac{\displaystyle\sum_{\mu=0}^{L-1} \mu^2 \sigma^2_{h,\,L-1-\mu} |z|^{2\mu}}{\displaystyle\sum_{\mu=0}^{L-1} \sigma^2_{h,\,L-1-\mu} |z|^{2\mu}} - \left(\frac{\displaystyle\sum_{\mu=0}^{L-1} \mu \sigma^2_{h,\,L-1-\mu} |z|^{2\mu}}{\displaystyle\sum_{\mu=0}^{L-1} \sigma^2_{h,\,L-1-\mu} |z|^{2\mu}} \right)^2 \right). \tag{29}$$

Note that for this special case the density of zeros $f_z(z)$ depends only on the magnitude $|z|$ of the complex variable z, i.e., it is rotational symmetric.[2] From (25) and (29), the marginal density $f_r(r)$ can be calculated to

$$f_r(r) = \frac{2}{r} \left(\frac{\displaystyle\sum_{\mu=0}^{L-1} \mu^2 \sigma^2_{h,\,L-1-\mu} r^{2\mu}}{\displaystyle\sum_{\mu=0}^{L-1} \sigma^2_{h,\,L-1-\mu} r^{2\mu}} - \left(\frac{\displaystyle\sum_{\mu=0}^{L-1} \mu \sigma^2_{h,\,L-1-\mu} r^{2\mu}}{\displaystyle\sum_{\mu=0}^{L-1} \sigma^2_{h,\,L-1-\mu} r^{2\mu}} \right)^2 \right). \tag{30}$$

For uncorrelated impulse response coefficients, it is also possible to obtain a closed-form result for the cumulative distribution functions $n(R)$ and $d(\rho)$. Using (26), (30) and basic integration rules, it can be shown easily that the expected number of zeros in the disc $|z| \le R$ is given by

$$n(R) = \frac{\displaystyle\sum_{\mu=0}^{L-1} \mu \sigma^2_{h,\,L-1-\mu} R^{2\mu}}{\displaystyle\sum_{\mu=0}^{L-1} \sigma^2_{h,\,L-1-\mu} R^{2\mu}}. \tag{31}$$

Finally, from (27) and (31)

$$\begin{aligned} d(\rho) &= \frac{\displaystyle\sum_{\mu=0}^{L-1} \mu \sigma^2_{h,\,L-1-\mu} \rho^{-2\mu}}{\displaystyle\sum_{\mu=0}^{L-1} \sigma^2_{h,\,L-1-\mu} \rho^{-2\mu}} - \frac{\displaystyle\sum_{\mu=0}^{L-1} \mu \sigma^2_{h,\,L-1-\mu} \rho^{2\mu}}{\displaystyle\sum_{\mu=0}^{L-1} \sigma^2_{h,\,L-1-\mu} \rho^{2\mu}} \\ &= \frac{\displaystyle\sum_{\mu=0}^{L-1} (L-1-\mu) \sigma^2_{h,\,\mu} \rho^{2\mu}}{\displaystyle\sum_{\mu=0}^{L-1} \sigma^2_{h,\,\mu} \rho^{2\mu}} - \frac{\displaystyle\sum_{\mu=0}^{L-1} \mu \sigma^2_{h,\,L-1-\mu} \rho^{2\mu}}{\displaystyle\sum_{\mu=0}^{L-1} \sigma^2_{h,\,L-1-\mu} \rho^{2\mu}} \end{aligned} \tag{32}$$

can be obtained. In the following, we further specialize the overall impulse response. More specifically, we consider impulse responses with exponentially increasing–decreasing and constant coefficient variances.

1) Exponentially Increasing–Decreasing Coefficient Variances: First, we assume that the coefficients of the overall impulse response have exponentially increasing–decreasing variances, i.e., $\sigma^2_{h,\,\mu} = \sigma^2_h e^{\beta\mu}$, $0 \le \mu \le L-1$, $\beta \in \mathbb{R}$. Such an exponential distribution of the overall channel coefficient variances is typical, e.g., for wireless communications in urban areas, e.g., [30]. In this case, the sums in (29) can be further simplified and the resulting density can be expressed as

$$f_z(z) = \frac{e^{-\beta}}{\pi} \frac{1 - \left(p_{L-1}\left(e^{-\beta}|z|^2\right)\right)^2}{\left(1 - e^{-\beta}|z|^2\right)^2} \tag{33}$$

with

$$p_{L-1}(x) = L\left(\sqrt{x}\right)^{L-1} \frac{1-x}{1-x^L}. \tag{34}$$

Furthermore, (30) can be simplified to

$$f_r(r) = 2e^{-\beta} r \frac{1 - \left(p_{L-1}(e^{-\beta} r^2)\right)^2}{(1 - e^{-\beta} r^2)^2} \tag{35}$$

and (31) yields

$$n(R) = \begin{cases} \dfrac{e^{-\beta} R^2}{1 - e^{-\beta} R^2} - L \dfrac{e^{-L\beta} R^{2L}}{1 - e^{-L\beta} R^{2L}}, & R \ne e^{\beta/2}. \\ \dfrac{L-1}{2}, & R = e^{\beta/2} \end{cases} \tag{36}$$

As was to be expected, $\lim_{R\to\infty} n(R) = L-1$ follows from (36). In addition, $n(R = e^{\beta/2}) = (L-1)/2$ implies that on average there are as many zeros inside the circle $r = e^{\beta/2}$ as outside this circle. This is a consequence of a general symmetry

[2]This result may be beneficial for the initialization of recursive algorithms for calculation of the zeros of polynomials, e.g., [28] and [29].

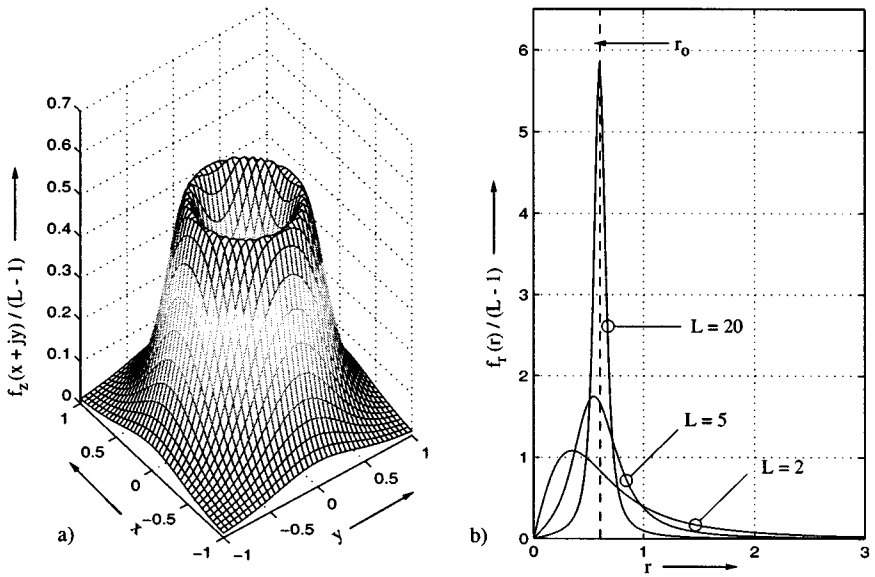

Fig. 2. (a) Normalized density of zeros $f_z(z)/(L-1)$ for $L=5$ and $\beta=-1$. (b) Normalized marginal density of zeros $f_r(r)/(L-1)$ for different impulse response lengths L and $\beta=-1$.

of $f_z(z)$ with respect to the circle $r=e^{\beta/2}$, i.e., $f_z(we^{\beta/2})=(1/|w|^2)f_z((1/w^*)e^{\beta/2})$, $w\in\mathbb{C}$, follows from (33).

Using (36), the relation

$$n(R)=L-1-n(e^{\beta}/R) \tag{37}$$

can be proved. From (26) and (37), the symmetry relations

$$\int_0^R f_r(r)\,dr=\int_{e^{\beta}/R}^{\infty} f_r(r)\,dr \tag{38}$$

and

$$\int_R^{e^{\beta/2}} f_r(r)\,dr=\int_{e^{\beta/2}}^{e^{\beta}/R} f_r(r)\,dr,\qquad 0<R\le e^{\beta/2} \tag{39}$$

follow directly. Equation (38) means that, for uncorrelated impulse response coefficients with exponentially increasing–decreasing variances, the average number of zeros in the regions $0\le|z|\le R$ and $e^{\beta}/R\le|z|<\infty$ are equal. According to (39), the same statement is true for the regions $R\le|z|\le e^{\beta/2}$ and $e^{\beta/2}\le|z|\le e^{\beta}/R$.

We now consider the expected number $b(\rho)$ of zeros in the region $\rho e^{\beta/2}\le|z|\le(1/\rho)e^{\beta/2}$, $0<\rho<1$

$$b(\rho)=n\left((1/\rho)e^{\beta/2}\right)-n(\rho e^{\beta/2}). \tag{40}$$

$b(\rho)$ can be calculated to

$$b(\rho)=L\frac{1+\rho^{2L}}{1-\rho^{2L}}-\frac{1+\rho^2}{1-\rho^2} \tag{41}$$

where (36) has been used. $\lim_{\rho\to 0}b(\rho)=L-1$ results, since integration is performed over the whole complex plane. For $L\gg 1$ and $\rho<1$, ρ^{2L} approaches zero. Thus, (41) simplifies to

$$b(\rho)\approx L-\frac{1+\rho^2}{1-\rho^2}=L-1-\frac{2\rho^2}{1-\rho^2}. \tag{42}$$

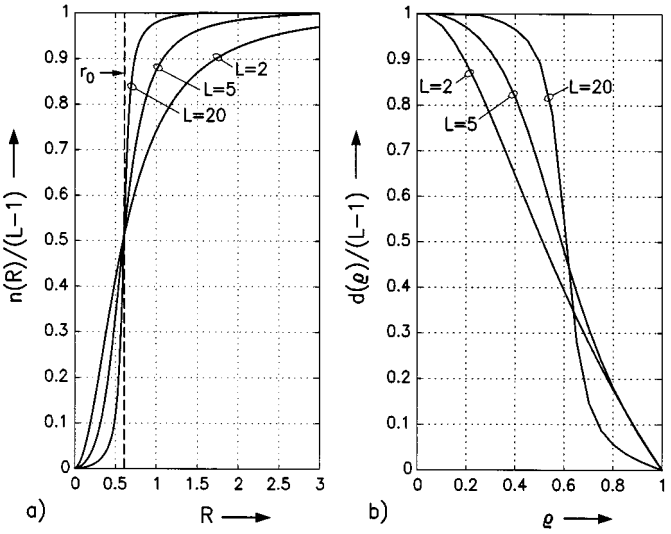

Fig. 3. (a) Normalized average number $n(R)/(L-1)$ of zeros inside the disc $|z|\le R$ for different impulse response lengths L and $\beta=-1$. (b) Normalized average number $d(\rho)/(L-1)$ of zeros inside the region $\rho\le|z|\le 1/\rho$ for different impulse response lengths L and $\beta=-1$.

This means that for long overall impulse responses, on average only $2\rho^2/(1-\rho^2)$ zeros are located outside the region $\rho e^{\beta/2}\le|z|\le(1/\rho)e^{\beta/2}$. For example, if $\rho=0.9$ is assumed, (42) yields $b(0.9)\approx L-9.5$. To become more specific, we assume $L=30$ and obtain 20.5 for the expected number of zeros in the region $0.9\,e^{\beta/2}\le|z|\le 1.11e^{\beta/2}$. From this example, we conclude that for very long impulse responses with uncorrelated zero mean coefficients having exponential variance distribution, most zeros are close to the circle $r=e^{\beta/2}$.

Hence, if β is considerably less or greater than zero, a significant complexity reduction is possible using impulse response truncation [9]–[14] since most zeros have a magnitude which is clearly different from one. Also, equalizer complexity may be reduced significantly using DFE or DDFSE/RSSE. For β con-

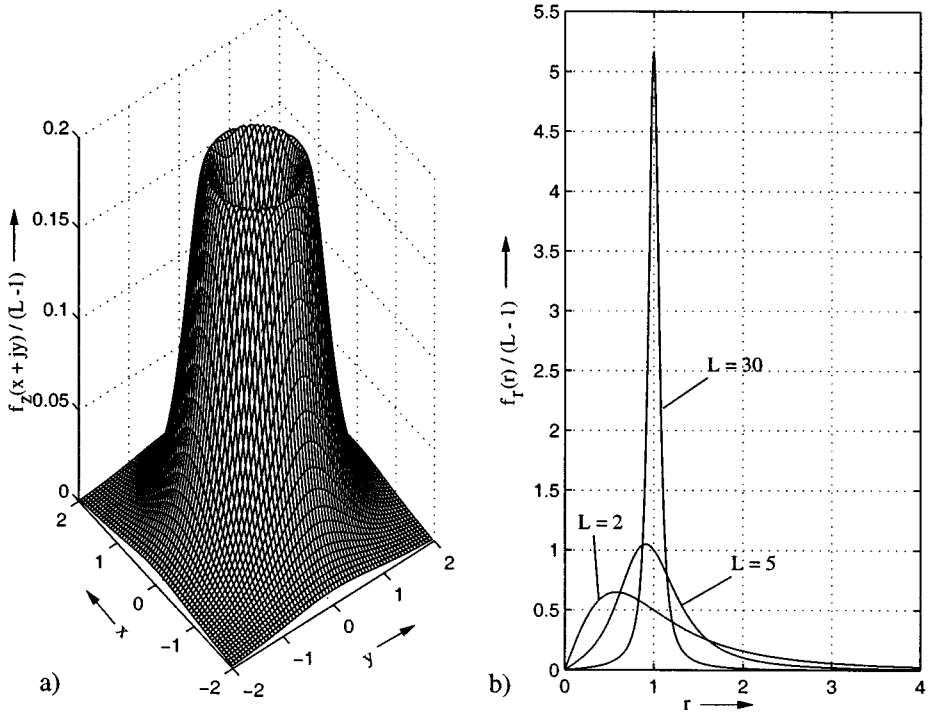

Fig. 4. (a) Normalized density of zeros $f_z(z)/(L-1)$ for $L = 5$. (b) Normalized marginal density of zeros $f_r(f)/(L-1)$ for different impulse response lengths L.

siderably less than zero, an additional minimum-phase transformation is not required, because the zeros are inside the unit circle with high probability. For β considerably greater than zero, the zeros are outside the unit circle with high probability, and prefiltering (see [26], [27], and [31]) is highly beneficial. Alternatively, reduced-state equalization may be applied in negative time direction (*backward decoding*) [32] in this case in order to avoid prefiltering. The important special case $\beta = 0$ will be discussed in the next paragraph.

In order to illustrate our results for uncorrelated impulse response coefficients with exponential variance distribution, Fig. 2(a) shows the (normalized) density $f_z(z = x+jy)/(L-1)$ for $\beta = -1$ and an impulse response length of $L = 5$. Clearly, uncorrelated zero mean coefficients cause a rotationally symmetric density. In Fig. 2(b), $f_r(r)/(L-1)$ is depicted for $\beta = -1$ and $L = 2$, 5, and 20. Note that for large L, $f_r(r)/(L-1)$ has a peak at $r = r_0 \triangleq e^{\beta/2} \approx 0.61$, i.e., the density of zeros is very high for $r = r_0$ and close to zero elsewhere. A similar observation can be made from the (normalized) cumulative distributions $n(R)/(L-1)$ and $d(\rho)/(L-1)$ which are shown in Fig. 3(a) and (b), respectively. Fig. 3(a) confirms that there are as many zeros outside the circle $r = r_0$ as inside.

2) Constant Coefficient Variances: Here, we assume that all taps of the overall impulse response have equal variance, i.e., $\sigma^2_{h,\nu} = \sigma^2_h, 0 \le \nu \le L-1$. All results of the previous paragraph can be applied if $\beta = 0$ is adopted.[3]

In particular, from (36) it can be observed that in this special case $n(R=1) = (L-1)/2$, i.e., on average there are as many zeros inside the unit circle as outside the unit circle. Thus, for uncorrelated impulse response coefficients having equal variance a minimum phase transformation is mandatory if DDFSE/RSSE is applied.

[3]Note that $n(R)$ for this special case can also be found in [33].

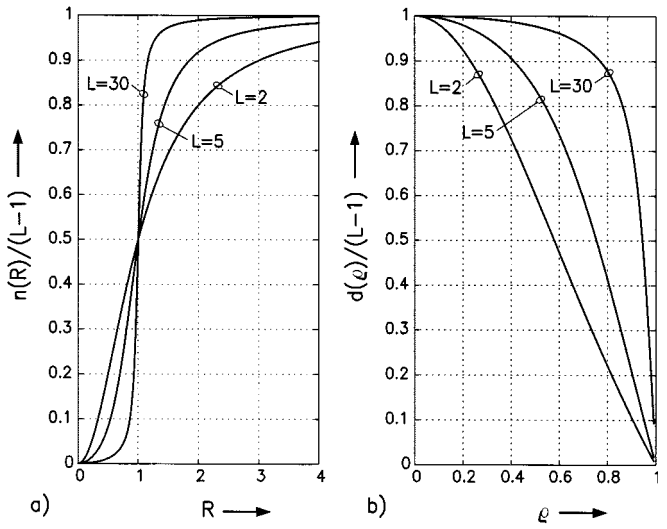

Fig. 5. (a) Normalized average number $n(R)/(L-1)$ of zeros inside the disc $|z| \le R$ for different impulse response lengths L. (b) Normalized average number $d(\rho)/(L-1)$ of zeros inside the region $\rho \le |z| \le 1/\rho$ for different impulse response lengths L.

Furthermore, for $\beta = 0$ $d(\rho) = b(\rho)$ holds. Therefore, $d(\rho)$ is given by (41) and (42) is the corresponding approximation for $L \gg 1$. From the considerations in the previous paragraph, it can be concluded that for very long impulse responses with approximately uncorrelated coefficients having equal variance

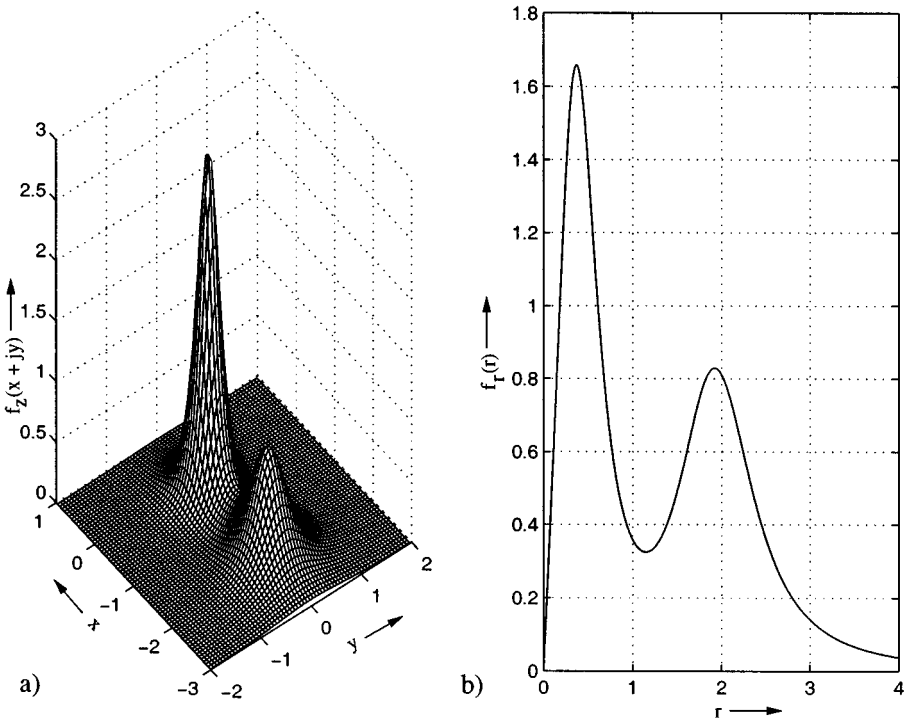

Fig. 6. (a) Unnormalized density of zeros $f_z(z)$. (b) Unnormalized marginal density of zeros $f_r(r)$ for the TU profile with $L = 3$.

(as they may be encountered, e.g., in underwater acoustic communications [34]), most zeros are close to the unit circle.[4] For example, for $L = 30$, the expected number of zeros in the region $0.9 \leq |z| \leq 1.11$ is 20.5. Therefore, the attainable complexity reduction using impulse response truncation [9]–[14] is limited since the truncated impulse response still has to be quite long (cf. Section IV-A). On the other hand, DFE and DDFSE/RSSE combined with a minimum phase transformation [26], [27] might be used. However, it should be noted that the effect of the minimum phase transformation is also limited. Since most zeros are close to the unit circle, transforming the zeros which are located outside the unit circle into it will not significantly increase the energy of the first coefficients of the overall impulse response. Therefore, also for DFE and DDFSE/RSSE a considerable loss in performance compared to MLSE has to be expected.

In order to illustrate our results for uncorrelated impulse response coefficients with equal tap variances, Fig. 4(a) shows the (normalized) density $f_z(z = x + jy)/(L-1)$ for an impulse response length of $L = 5$. In Fig. 4(b), $f_r(r)/(L-1)$ is depicted for $L = 2$, 5, and 30. Now $f_r(r)/(L-1)$ has a peak at $r = 1$ for large L. The (normalized) cumulative distributions $n(R)/(L-1)$ and $d(\rho)/(L-1)$ are shown in Fig. 5(a) and (b), respectively. Fig. 5(a) confirms that there are as many zeros outside the unit circle as inside, while Fig. 5(b) illustrates that for $L = 2$ and $L = 5$ on average only 10% and 20% of all zeros lie in the region $0.9 \leq |z| \leq 1.11$, respectively. For $L = 30$, however, more than 70% of all zeros lie in this region and impulse response truncation is not expected to perform well unless the truncated impulse response is quite long.

[4]We would like to mention that a similar observation has been made before in the engineering literature [35].

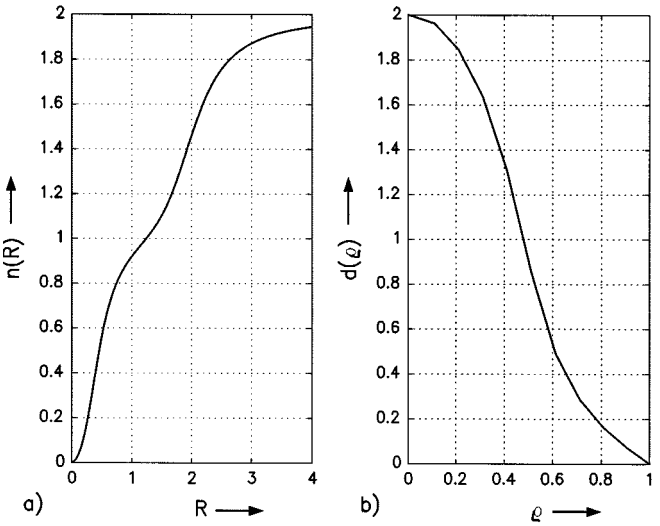

Fig. 7. (a) Average number $n(R)$ of zeros inside the disc $|z| \leq R$. (b) Average number $d(\rho)$ of zeros in the region $\rho \leq |z| \leq 1/\rho$ for the TU profile with $L = 3$.

V. Results for GSM/EDGE Power Delay Profiles

For the GSM/EDGE system, four different power delay profiles are specified [23]: rural area (RA), hilly terrain (HT), typical urban area (TU), and equalizer test (EQ). For HT, TU, and EQ, it is assumed that the amplitudes of all propagation paths are zero-mean complex Gaussian random variables and, thus, the distribution of zeros of the corresponding overall transfer functions may be analyzed using the methods presented in the previous sections. Note that the channel specified for RA is essentially flat, i.e., the zeros of the overall transfer function are mainly influenced by transmit and receiver input filter.

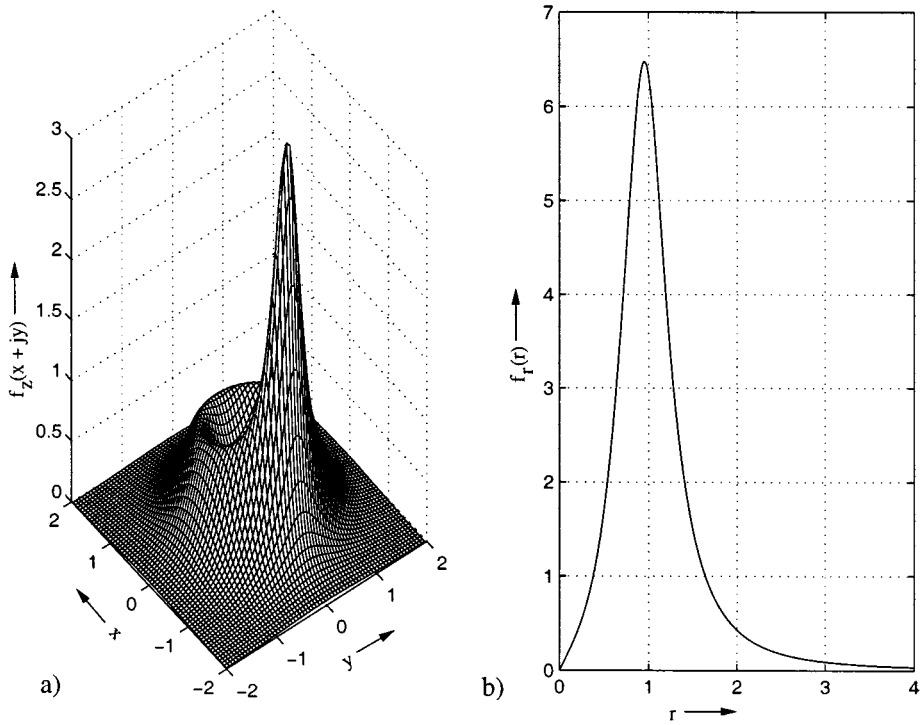

Fig. 8. (a) Unnormalized density of zeros $f_z(z)$. (b) Unnormalized marginal density of zeros $f_r(r)$ for the EQ profile with $L = 6$.

For calculation of the correlation matrix $\boldsymbol{C}$ transmit and receiver input filter impulse response are required. For the transmit filter $h_T(t)$ a linearized Gaussian minimum phase-shift keying (GMSK) pulse [36], [37] is standardized for EDGE in order to obtain full compatibility with GSM where GMSK modulation is employed [4]. Thus, the linearized GMSK pulse is also used in this paper. The choice of the receiver input filter $h_R(t)$ is up to the receiver designer. Here, we use a fixed filter, namely a square-root raised cosine (SRC) filter with roll-off factor 0.3 [20]. This filter offers a similar performance like the optimum whitened matched filter (WMF) [1]. However, the implementation of the SRC filter is much simpler since, in contrast to the WMF, it does not have to be adapted to a particular channel impulse response [5]. The power delay profiles are taken from [23] [for HT and TU alternative (1) is used, respectively]. The sampling phase $\hat{t}_0$ is determined as described in Section II (11). As already mentioned, now $f_r(r)$, $n(R)$, and $d(\rho)$ cannot be calculated in closed form but have to be obtained by numerical integration.

Figs. 6 and 7 show the results for the TU profile. The overall impulse response was truncated to $L = 3$ taps. This leads to a precursor energy of $E_{\mathrm{pre}}(\hat{t}_0) = 3{\cdot}10^{-4}$ and a postcursor energy of $E_{\mathrm{post}}(\hat{t}_0) = 3 \cdot 10^{-3}$. Note that the total energy $E(\hat{t}_0)$ was normalized to 1. If L was chosen larger there would be taps containing very little energy and this would cause additional zeros with very small or/and very large magnitudes. Fig. 6(a) clearly illustrates that in contrast to the case of uncorrelated impulse response coefficients, the density of zeros $f_z(z)$ is not rotational symmetric. This is because transmit and receiver input filter introduce correlations between different impulse response coefficients, i.e., $\boldsymbol{C}$ is not a diagonal matrix. Fig. 6(b) shows that $f_r(r)$ has a local minimum close to $r = |z| = 1$. Thus, impulse response truncation may be employed successfully. However, the obtainable decrease in complexity is moderate since the truncated impulse response should still have a length of 2. On average, 0.07 zeros are located in the region $0.9 \leq |z| \leq 1.11$ [cf. Fig. 7(b)]. From this, we conclude that it is unlikely that two zeros of the overall impulse response are close to the unit circle but the case that one zero is close to the unit circle will occur more frequently and thus, truncating the overall impulse response to a length of one (i.e., performing linear equalization) causes considerable degradation. DFE and DDFSE/RSSE

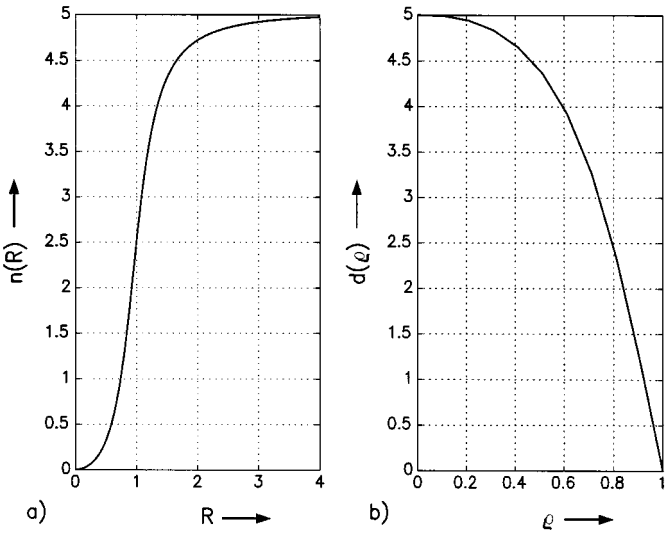

Fig. 9. (a) Average number $n(R)$ of zeros inside the disc $|z| \leq R$. (b) Average number $d(\rho)$ of zeros in the region $\rho \leq |z| \leq 1/\rho$ for the EQ profile with $L = 6$.

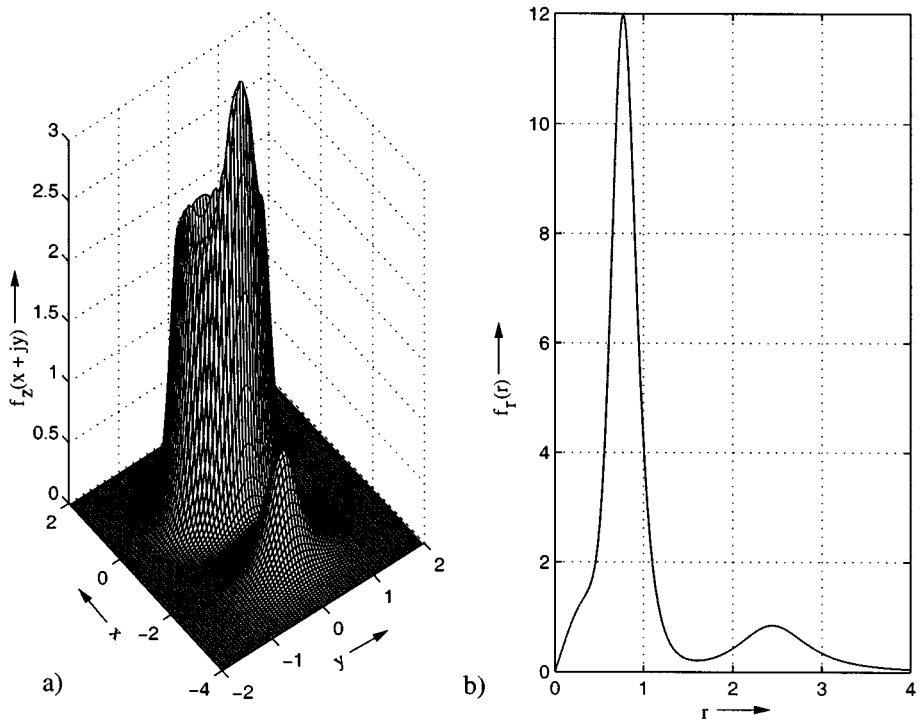

Fig. 10. (a) Unnormalized density of zeros $f_z(z)$. (b) Unnormalized marginal density of zeros $f_r(r)$ for the HT profile with $L = 7$.

techniques should only be employed in combination with an appropriate allpass prefilter which transforms the overall impulse response in its minimum phase equivalent. This follows from Fig. 7(a), which shows that, on average, 1.1 zeros are located outside the unit circle.

In Figs. 8 and 9, the EQ profile is considered. Here, for the length of the overall impulse response, $L = 6$ is chosen. This results in precursor and postcursor energies of $E_{\mathrm{pre}}(\hat{t}_0) = 1{\cdot}10^{-3}$ and $E_{\mathrm{post}}(\hat{t}_0) = 1 \cdot 10^{-3}$, respectively. Fig. 8(a) shows that $f_z(z)$ has a peak at approximately $z = -1$. Note that a zero at $z = -1$ results if, e.g., $h[0, \hat{t}_0]$ and $h[1, \hat{t}_0]$, $h[2, \hat{t}_0]$ and $h[3, \hat{t}_0]$, and $h[4, \hat{t}_0]$ and $h[5, \hat{t}_0]$ are equal, respectively. Due to the strong correlations (introduced by transmit and receiver input filter) between neighboring taps of the overall impulse response, it is quite likely that neighboring taps are approximately equal which leads to the peak of $f_z(z)$ at $z = -1$. Note also that the correlation between neighboring taps is more pronounced for the EQ profile than for the TU and HT profiles since for EQ all six paths have equal energy [23]. From Fig. 9(a), it can be observed that for EQ there are on average as many zeros inside the unit circle as outside. Thus, for application of DFE and DDFSE/RSSE, an allpass prefilter which transforms the overall impulse response in its minimum phase equivalent should be applied. Fig. 9(b) implies that, on average, there are 1.2 zeros in the region $0.9 \leq |z| \leq 1.1$. Thus, for impulse response truncation, the resulting overall impulse response should have at least a length of 3 (i.e., two zeros) in order to avoid excessive noise enhancement.

Finally, in Figs. 10 and 11, the HT profile is considered. The length of the overall impulse response is $L = 7$ which leads to a precursor energy of $E_{\mathrm{pre}}(\hat{t}_0) = 3{\cdot}10^{-4}$ and a postcursor energy of $E_{\mathrm{post}}(\hat{t}_0) = 2 \cdot 10^{-3}$. Although Fig. 10(a) and (b) clearly show that most zeros are located inside the unit circle, Fig. 11(a) shows that on average 0.8 zeros are located in the area $|z| \geq 2$. Transforming these zeros inside the unit circle will enhance the energy of the first taps of the impulse response considerably and, thus, improve the performance of DFE and DDFSE/RSSE schemes significantly. Hence, we also recommend the use of an allpass prefilter for HT. It can be observed from Fig. 11(b) that on average only one zero lies in the region $0.9 \leq |z| \leq 1.1$. Therefore, we expect that the overall impulse response can be truncated (via a suitable prefilter) to a length of 3 without significant loss in performance.

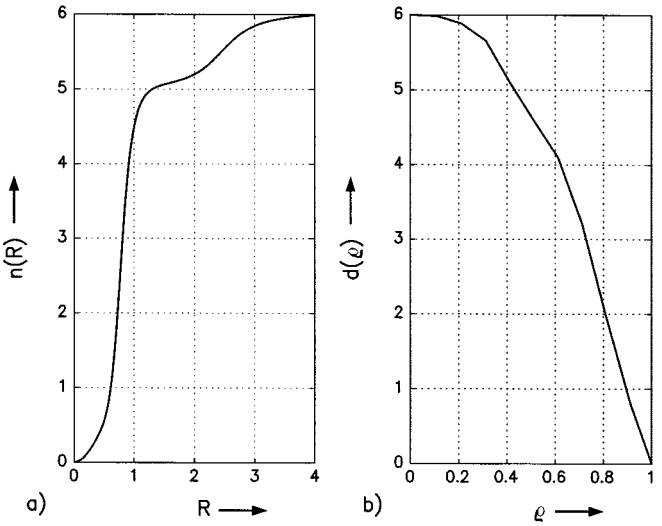

Fig. 11. (a) Average number $n(R)$ of zeros inside the disc $|z| \leq R$. (b) Average number $d(\rho)$ of zeros in the region $\rho \leq |z| \leq 1/\rho$ for the HT profile with $L = 7$.

VI. Conclusion

In this paper, the distribution of zeros of mobile channels characterized by a power delay profile is analyzed. The taps of the discrete-time overall impulse response of mobile channels can be described as correlated Gaussian random variables where the correlation between taps depends on the transmit filter, the equivalent baseband channel power delay profile, and the receiver input filter. Using a result from the mathematical literature, the density of zeros of the overall transfer function is calculated in closed form. From this density, two cumulative distributions are derived and their importance for the design of suboptimum receivers is shown.

For the special case that all taps of the overall impulse response are mutually uncorrelated, closed-form expressions for both cumulative distributions are obtained. In addition, it turns out that for long impulse responses with uncorrelated taps with exponentially increasing (decreasing) variances the zeros concentrate on a circle with a radius larger (smaller) than one. It is also shown that for uncorrelated taps with equal energy there are as many zeros inside the unit circle as outside and that especially for long impulse responses most zeros are located close to the unit circle. Therefore, it can be concluded that in this case for moderate impulse response lengths an allpass prefilter should be used for DFE and DDFSE/RSSE whereas for very long impulse responses the allpass filter will not significantly increase the energy of the first taps of the overall impulse response. If impulse response truncation using a prefilter is employed, the truncated impulse response still has to be quite long in order to avoid noise enhancement.

Finally, the power delay profiles specified for GSM/EDGE are investigated in this paper. It is shown that if DFE or DDFSE/RSSE are employed, an allpass prefilter should be inserted for all profiles. In addition, it turned out that for impulse response truncation a length of 3 of the truncated impulse response is sufficient in all cases.

Appendix

In this appendix, $f_z(z)$ is calculated from (19). Using (15), (19) may be rewritten to

$$f_z(z) = \frac{1}{\pi} \frac{\partial^2}{\partial z \partial z^*} \log \left(\sum_{\mu=0}^{L-1} \sum_{\nu=0}^{L-1} c_{\mu\nu} z^{\mu} (z^*)^{\nu} \right). \tag{43}$$

For differentiation with respect to z, z^* has to be considered as a constant [24]. Thus,

$$f_z(z) = \frac{1}{\pi} \frac{\partial}{\partial z^*} \frac{\sum_{\mu=0}^{L-1} \sum_{\nu=0}^{L-1} \mu c_{\mu\nu} z^{(\mu-1)} (z^*)^{\nu}}{\sum_{\mu=0}^{L-1} \sum_{\nu=0}^{L-1} c_{\mu\nu} z^{\mu} (z^*)^{\nu}} \tag{44}$$

is obtained. Performing also the differentiation with respect to z^* yields

$$f_z(z) = \frac{1}{\pi |z|^2} \left(\frac{\sum_{\mu=0}^{L-1} \sum_{\nu=0}^{L-1} \mu\nu c_{\mu\nu} z^{\mu} (z^*)^{\nu}}{\sum_{\mu=0}^{L-1} \sum_{\nu=0}^{L-1} c_{\mu\nu} z^{\mu} (z^*)^{\nu}} - \frac{\sum_{\mu=0}^{L-1} \sum_{\nu=0}^{L-1} \mu c_{\mu\nu} z^{\mu} (z^*)^{\nu} \sum_{\mu=0}^{L-1} \sum_{\nu=0}^{L-1} \nu c_{\mu\nu} z^{\mu} (z^*)^{\nu}}{\left(\sum_{\mu=0}^{L-1} \sum_{\nu=0}^{L-1} c_{\mu\nu} z^{\mu} (z^*)^{\nu} \right)^2} \right). \tag{45}$$

Since $\boldsymbol{C}$ is a Hermitian matrix, $c_{\mu\nu} = c_{\nu\mu}^*$, $0 \leq \nu, \mu \leq L-1$, holds and $\sum_{\mu=0}^{L-1} \sum_{\nu=0}^{L-1} \nu c_{\mu\nu} z^{\mu} (z^*)^{\nu} = (\sum_{\mu=0}^{L-1} \sum_{\nu=0}^{L-1} \mu c_{\mu\nu} z^{\mu} (z^*)^{\nu})^*$ is valid. Using this relation in (45) it is straightforward to show that (20)–(24) are true.

References

[1] G. D. Forney Jr., "Maximum-likelihood sequence estimation of digital sequences in the presence of intersymbol interference," *IEEE Trans. Inform. Theory*, vol. IT-18, pp. 363–378, May 1972.

[2] G. Ungerböck, "Adaptive maximum-likelihood receiver for carrier-modulated data-transmission systems," *IEEE Trans. Commun.*, vol. COM-22, pp. 624–636, May 1974.

[3] G. D. Forney Jr., "The Viterbi algorithm," *IEEE Proc.*, vol. 61, pp. 268–278, Mar. 1973.

[4] A. Furuskär, S. Mazur, F. Müller, and H. Olofsson, "EDGE: Enhanced data rates for GSM and TDMA/136 evolution," *IEEE Pers. Commun. Mag.*, vol. 6, pp. 56–66, June 1999.

[5] W. H. Gerstacker and R. Schober, "Equalization concepts for EDGE," *Electron. Lett.*, vol. 36, pp. 189–191, Jan. 2000.

[6] W. Koch and A. Baier, "Optimum and sub-optimum detection of coded data disturbed by time-varying intersymbol interference," in *Proc. IEEE Global Telecommunication Conf.*, San Diego, CA, Dec. 1990, pp. 807.5.1–807.5.6.

[7] A. Duel-Hallen and A. C. Heegard, "Delayed decision-feedback sequence estimation," *IEEE Trans. Commun.*, vol. COM-37, pp. 428–436, May 1989.

[8] M. V. Eyuboğlu and S. U. Qureshi, "Reduced-state sequence estimation with set partitioning and decision feedback," *IEEE Trans. Commun.*, vol. COM-36, pp. 13–20, Jan. 1988.

[9] S. U. H. Qureshi and E. E. Newhall, "An adaptive receiver for data transmission over time-dispersive channels," *IEEE Trans. Inform. Theory*, vol. IT-19, pp. 448–457, July 1973.

[10] D. D. Falconer Jr. and F. R. Magee, "Adaptive channel memory truncation for maximum-likelihood sequence estimation," *Bell Syst. Technol. J.*, vol. 52, pp. 1541–1562, Nov. 1973.

[11] C. T. Beare, "The choice of the desired impulse response in combined linear-Viterbi algorithm equalizers," *IEEE Trans. Commun.*, vol. COM-26, pp. 1301–1327, Aug. 1978.

[12] K. D. Kammeyer, "Time truncation of channel impulse responses by linear filtering: A method to reduce the complexity of Viterbi equalization," *Int. J. Electron. Commun.*, vol. 48, no. 5, pp. 237–243, 1994.

[13] I. L. Lee and J. M. Cioffi, "Design of equalized maximum-likelihood receiver," *IEEE Commun. Lett.*, vol. 2, pp. 14–16, Jan. 1998.

[14] M. Magarini, A. Spalvieri, and G. Tartara, "Improving error performance of equalized receivers for broadband radio," in *IEEE Vehicular Technology Conf.*, Amsterdam, The Netherlands, Sept. 1999, pp. 2377–2381.

[15] C. A. Belifiore and J. H. Park, "Decision-feedback equalization," *Proc. IEEE*, vol. 67, pp. 1143–1156, Aug. 1979.
[16] R. W. Lucky, J. Salz Jr., and E. J. Weldon, *Principles of Data Communication*. New York: McGraw-Hill, 1968.
[17] E. J. Borowski and J. M. Borwein, *The Harper Collins Dictionary of Mathematics*. New York: Harper Perennial, 1991.
[18] J. G. Proakis, *Digital Communications*, 3rd ed. New York: McGraw-Hill, 1995.
[19] M. Gagnaire, "An overview of broad-band access technologies," *Proc. IEEE*, vol. 85, no. 12, pp. 1958–1972, Dec. 1997.
[20] T. S. Rappaport, *Wireless Communications*. Englewood Cliffs, NJ: Prentice-Hall, 1996.
[21] A. Edelman and E. Kostlan, "How many zeros of a random polynomial are real," *Bull. Amer. Math. Soc.*, vol. 32, pp. 1–37, Jan. 1995.
[22] J. M. Hammersley, "The zeros of a random polynomial," in *Proc. 3rd Berkeley Symp. Mathematical Statistics and Probability*, CA, 1956, pp. 89–111.
[23] "Propagation conditions,", GSM Recommendation 05.05, Vers. 5.3.0, Release, 1996.
[24] V. S. Vladimirov, *Methods of the Theory of Functions of Many Complex Variables*. Cambridge, MA: M.I.T. Press, 1964.
[25] A. Papoulis, *Probability, Random Variables and Stochastic Processes*. New York: McGraw-Hill, 1984.
[26] W. Gerstacker and J. Huber, "Improved equalization for GSM mobile communications," in *Proc. Int. Conf. Telecommunications*, Istanbul, Turkey, Apr. 1996, pp. 128–131.
[27] M. Schmidt and G. P. Fettweis, "FIR prefiltering for near minimum phase target channels," presented at the 6th Canadian Workshop Information Theory, Kingston, ON, Canada, June 1999.
[28] Y. Nagashima, T. Kanda, and H. Nagashima, "Improvement on Aberth's method for choosing initial approximations to zeros of polynomials," *IEE Proceedings E*, vol. 136, pp. 101–106, Mar. 1989.
[29] O. Aberth, "Iteration methods for finding all zeros of a polynomial simultaneously," *Math. Comput.*, vol. 27, pp. 339–344, 1973.
[30] "Digital land mobile radio communications. Final report," Office for Official Publications of the European Communities, Luxemburg, COST 207, 1989.
[31] W. Gerstacker, F. Obernosterer, R. Meyer, and J. Huber, "An efficient method for prefilter computation for reduced-state equalization," in *Proc. Int. Symp. Personal, Indoor and Mobile Radio Communication*, London, U.K., Sept. 2000, pp. 604–609.
[32] K. Balachandran and J. B. Anderson, "Reduced complexity sequence detection for nonminimum phase intersymbol interference channels," *IEEE Trans. Inform. Theory*, vol. IT-43, pp. 275–280, Jan. 1997.
[33] L. Arnold, "Über die Nullstellenverteilung zufälliger Polynome (in German)," *Math. Zeitschrift*, vol. 92, pp. 12–18, 1966.
[34] A. Falahati, B. Woodward, and S. C. Bateman, "Underwater acoustic channel models for 4800 b/s QDPSK signals," *IEEE J. Oceanic Eng.*, vol. 16, pp. 12–20, Jan. 1991.
[35] K. Steiglitz and B. Dickinson, "Phase unwrapping by factorization," *IEEE Trans. Acoust., Speech, Signal Processing*, vol. ASSP-30, pp. 984–991, Dec. 1982.
[36] P. Jung, "Laurent's representation of binary continuous phase modulated signals with modulation index 1/2 revisited," *IEEE Trans. Commun.*, vol. 42, pp. 221–224, Feb. 1994.
[37] *Introduction of 8PSK*: Source Ericsson, 1999.

Robert Schober (S'98) was born in Neuendettelsau, Germany, in 1971. He received the Diplom (Univ.) degree in electrical engineering from the University of Erlangen-Nürnberg in October 1997. During his studies, he was supported by a scholarship of the "Studienstiftung des deutschen Volkes." In June 2000, he received the Dr. Ing. degree with a thesis on noncoherent detection and equalization.

From November 1997 to May 2001, he was a Research Assistant with the Telecommunications Institute II (Digital Transmission and Mobile Communications), University of Erlangen-Nürnberg. Since May 2001, he has been a Visiting Research Fellow with the University of Toronto, sponsored by a fellowship from the German Academic Exchange Service (DAAD). His main research interests are in the area of noncoherent detection, equalization, and multiuser detection.

Wolfgang H. Gerstacker (S'93–M'99) was born in Nürnberg, Germany, in 1966. He received the Dipl.-Ing. degree in electrical engineering from the University of Erlangen-Nürnberg in 1991. In 1998, he received the Dr.-Ing. degree with a thesis on improved equalization concepts for transmission over twisted pair lines.

From 1992 to 1998, he was a Research Assistant with the Telecommunications Institute, University of Erlangen-Nürnberg. Since 1998, he has been a consultant working in the area of mobile communications and also performing joint work with the Telecommunications Institute II, University of Erlangen-Nürnberg. In 1999/2000, he was a Visiting Research Fellow for a six months period with the University of Canterbury, Christchurch, New Zealand, sponsored by a fellowship from DAAD. His research interests are (adaptive) equalization for high-rate baseband transmission schemes, such as xDSL, equalization and channel estimation for mobile communications systems, blind equalization, and noncoherent detection algorithms.